Title: Waves of chromatin modifications in mouse dendritic cells in response to LPS stimulation

Authors: Alexis Vandenbon[1$]*, Yutaro Kumagai[2$], Mengjie Lin[3], Yutaka Suzuki[3], Kenta Nakai[4]*

[1] Immuno-Genomics Research Unit, Immunology Frontier Research Center (IFReC), Osaka University, Suita, 565-0871, Japan

[2] Quantitative Immunology Research Unit, Immunology Frontier Research Center (IFReC), Osaka University, Suita, 565-0871, Japan

[3]Department of Computational Biology and Medical Sciences, Graduate School of Frontier Sciences, The University of Tokyo, Kashiwa 277-8561, Japan

[4] Laboratory of Functional Analysis in silico, The Institute of Medical Science, The University of Tokyo, Minato-ku, Tokyo, 108-8639, Japan

$ Equal contribution

* To whom correspondence should be addressed. Email: alexisvdb@ifrec.osaka-u.ac.jp, knakai@ims.u-tokyo.ac.jp

Abstract

Background: The importance of transcription factors (TFs) and epigenetic modifications in the control of gene expression is widely accepted. However, causal relationships between changes in TF binding, histone modifications, and gene expression during the response to extracellular stimuli are not well understood. Here, we analyzed the ordering of these events on a genome-wide scale in dendritic cells (DCs) in response to lipopolysaccharide (LPS) stimulation.

Results: We found that LPS-induced increases in several histone modifications at promoters and enhancers occur in "waves" within specific time frames after stimulation, independent of the timing of transcriptional induction. Integrative analysis with TF binding data revealed potential links between the timing of TF binding and accumulation of histone modifications. Especially, binding by STAT1/2 coincided with induction of H3K9K14ac, and was followed by increases in H3K4me3. In a subset of LPS-induced genes the induction of these modifications was found to be TRIF-, IRF3-, and IFNR-dependent, further supporting a possible role for STAT1/2 in the regulation of these histone modifications.

Conclusions: The timing of stimulus-induced, short-term changes in histone modifications appears to be relatively independent of dynamics in activity of regulatory regions. This suggests a lack of a direct causal relationship. Changes in modifications more likely reflect the activation of stimulus-dependent TFs and their interactions with chromatin modifiers.

Running title: Waves of chromatin modification in immune response

Keywords: histone modifications, dendritic cells, epigenetics, transcription factors

Introduction

Epigenetic features, such as covalent post-translational modifications of histone proteins and DNA methylation, are thought to play a crucial role in controlling the accessibility of DNA to RNA polymerases. Associations have been found between histone modifications and both long-term and short-term cellular processes, including development, heritability of cell type identity, DNA repair, and transcriptional control (Henikoff 2008; Greer and Shi 2012). For cells of the hematopoietic lineage, cell type-defining enhancers are thought to be established during the process of differentiation from stem cells by priming with the H3K4me1 marker (Mercer et al. 2011; Winter and Amit 2014). On the other hand, in differentiated cells, extracellular stimuli are accompanied by relatively short-term or transient changes in histone modifications reflecting the changes in activity of enhancers and promoters (Creyghton et al. 2010; Kaikkonen et al. 2013; Ostuni et al. 2013).

TFs are key regulators in the control of epigenetic changes (Voss and Hager 2014; Álvarez-Errico et al. 2014). During the long-term process of development, closed chromatin is first bound by pioneer TFs, which results in structural changes that make it accessible to other TFs and RNA polymerase II (Pol2) (Heinz et al. 2010; Ostuni et al. 2013). Similarly, more short-term changes in gene expression following stimulation of immune cells are regulated by TFs. This regulation is thought to involve TF binding, induction of changes in histone modifications, and recruitment of Pol2 (Foster et al. 2007; Smale et al. 2014; Ghisletti et al. 2010; Natoli 2009). However, details of the temporal ordering and causal relationships between these events remain poorly understood (Henikoff and Shilatifard 2011; Ivashkiv and Park 2016). Especially, it is unclear whether certain histone modifications are a requirement for, or just a result of, TF binding and transcription (Miller et al. 2001; Pavri et al. 2006; Stasevich et al. 2014).

As sentinel cells of the innate immune system, DCs are well equipped for detecting the presence of pathogens. Lipopolysaccharide (LPS), a component of the cell wall of Gram negative bacteria, is recognized by DCs through the membrane-bound Toll-like receptor 4 (TLR4), resulting in the

activation of two downstream signaling pathways (Kawai and Akira 2010). One pathway is dependent on the adaptor protein MyD88, and leads to the activation of the TF NF-κB, which induces expression of proinflammatory cytokines. The other pathway involves the receptor protein TRIF, whose activation induces phosphorylation of the TF IRF3 by TBK1 kinase. The activated IRF3 induces expression of type I interferon, which in turn activates the JAK-STAT signaling pathway, by binding to the type I IFN receptor (IFNR) (Hoshino et al. 2002).

Here, we present a large-scale study of short-term changes in histone modifications in mouse DCs during the response to LPS. We focused on the timing of changes in histone modifications at promoters and enhancers, relative to the induction of transcription and to TF binding events. We observed that LPS stimulation induced increased levels of H3K9K14ac, H3K27ac, H3K4me3 and H3K36me3 at LPS-induced promoters and enhancers. However, surprisingly, we found that the induction of H3K9K14ac (between 0.5 and 3 hours), H3K4me3 (between 2 and 4 hours), and H3K36me3 (between 8 and 24 hours) occurred within specific time frames after stimulation, independent of the timing of transcriptional induction of nearby genes. This finding suggests a lack of a direct causal relation between increases in these markers and induction of gene expression. Integrated analysis of induction times of histone modifications with genome-wide binding data for 24 TFs revealed possible associations between increases in H3K9K14ac and H3K4me3 and binding by Rela, Irf1, and especially STAT1/2. For STAT1/2, this association was further supported using independent ChIP-qPCR experiments in $TRIF^{-/-}$, $IRF3^{-/-}$, and $IFNR^{-/-}$ cells, and in wild type (WT) and $TRIF^{-/-}$ cells stimulated with IFN-β. Together, these results suggest that waves of histone modification changes might reflect the timing of activation of stimulus-dependent TFs, and complex interactions between TFs and epigenetic modifiers in the control of gene expression.

Results

Genome-wide Measurement of Histone Modifications at Promoter and Enhancer Regions

To elucidate the temporal ordering of stimulus-induced changes in transcription and chromatin structure, we performed chromatin immunoprecipitation experiments followed by high-throughput sequencing (ChIP-seq) for the following histone modifications in mouse DCs before and after LPS stimulation: H3K4me1, H3K4me3, H3K9K14ac, H3K9me3, H3K27ac, H3K27me3, H3K36me3, and similarly for Pol2 (Fig. S1), for ten time points (0h, 0.5h, 1h, 2h, 3h, 4h, 6h, 8h, 16h, 24h). We integrated this data with publicly available whole-genome transcription start site (TSS) data (TSS-seq) (Liang et al. 2014). All data originated from the same cell type, treated with the same stimulus, and samples taken at the same time points.

Using this data collection, we defined 24,416 promoters (based on TSS-seq data and Refseq annotations) and 34,079 enhancers (using H3K4me1^{high}/H3K4me3^{low} signals) (see Methods). For this genome-wide set of promoters and enhancers, we estimated the levels of histone modifications, Pol2 binding, and RNA reads over time (see Methods).

Epigenetic Changes at Inducible Promoters and their Enhancers

Recent studies using the same cell type and stimulus showed that most changes in gene expression patterns were controlled at the transcriptional level, without widespread changes in RNA degradation rates (Rabani et al. 2014; Kumagai et al.). We therefore defined 1,413 LPS-induced promoters based on increases in TSS-seq reads after LPS stimulation, and inferred their transcriptional induction time (see Methods). Fig. 1A shows changes in transcriptional activity of LPS-induced promoters. In addition to a relatively large number of immediate-early induced promoters (0.5h, 259 promoters) and promoters with very late induction (24h, 299 promoters), at each time

point we observed between 85 to 180 induced promoters. In addition, we defined a set of 772 promoters with highly stable activity over the entire time course (see Methods).

A previous study suggested only limited dynamics of histone modifications at stimulus-induced promoters in mouse DCs, based on data taken at a few time points (Garber et al. 2012). Our dataset, however, allows the analysis of the timing of changes over an extended time period after stimulation.

For both promoters and enhancers, we defined significant increases in histone modifications and Pol2 binding by comparison to pre-stimulation levels (see Methods). Our analysis suggested that changes were in general rare; only 0.7 to 5.3 % of all promoters (Fig. 1B) and 0.2 to 11.0 % of all enhancers (Fig. 1C) experienced significant increases in histone modifications and Pol2 binding. Changes at the promoters and enhancers of stably active promoters were similarly rare (not shown). However, changes were found relatively frequently at LPS-induced promoters, especially for markers of activity such as Pol2 binding, H3K4me3, H3K27ac, and H3K9K14ac, as well as for H3K36me3 (Fig. 1B). For example, while only 957 promoters (out of a total of 24,416 promoters; 3.9%) experienced significant increases in H3K9K14ac, this included 27.6% of the LPS-induced promoters (390 out of 1,413 promoters). To a lesser extent, we observed the same tendency at associated enhancers (Fig. 1C). The smaller differences at enhancers are likely to be caused by imperfect assignments of enhancers to LPS-induced promoters (i.e. we naively assigned enhancers to their most proximal promoter).

LPS-induced promoters were less frequently associated with CpG islands (57%) than stably expressed promoters (87%, Fig. S2A) (Illingworth and Bird 2009). Non-CpG promoters more frequently had lower basal levels (i.e. levels at 0h, before stimulation) of activation-associated histone modifications, such as H3K27ac, H3K9K14ac, H3K4me3, and similarly lower levels of Pol2 binding and pre-stimulation gene expression (Fig. S2B). This partly explains the higher frequency of

significant increases in histone modifications at LPS-induced promoters (Fig. S2B), and the higher fold-induction of genes associated with non-CpG promoters (Fig. S2C).

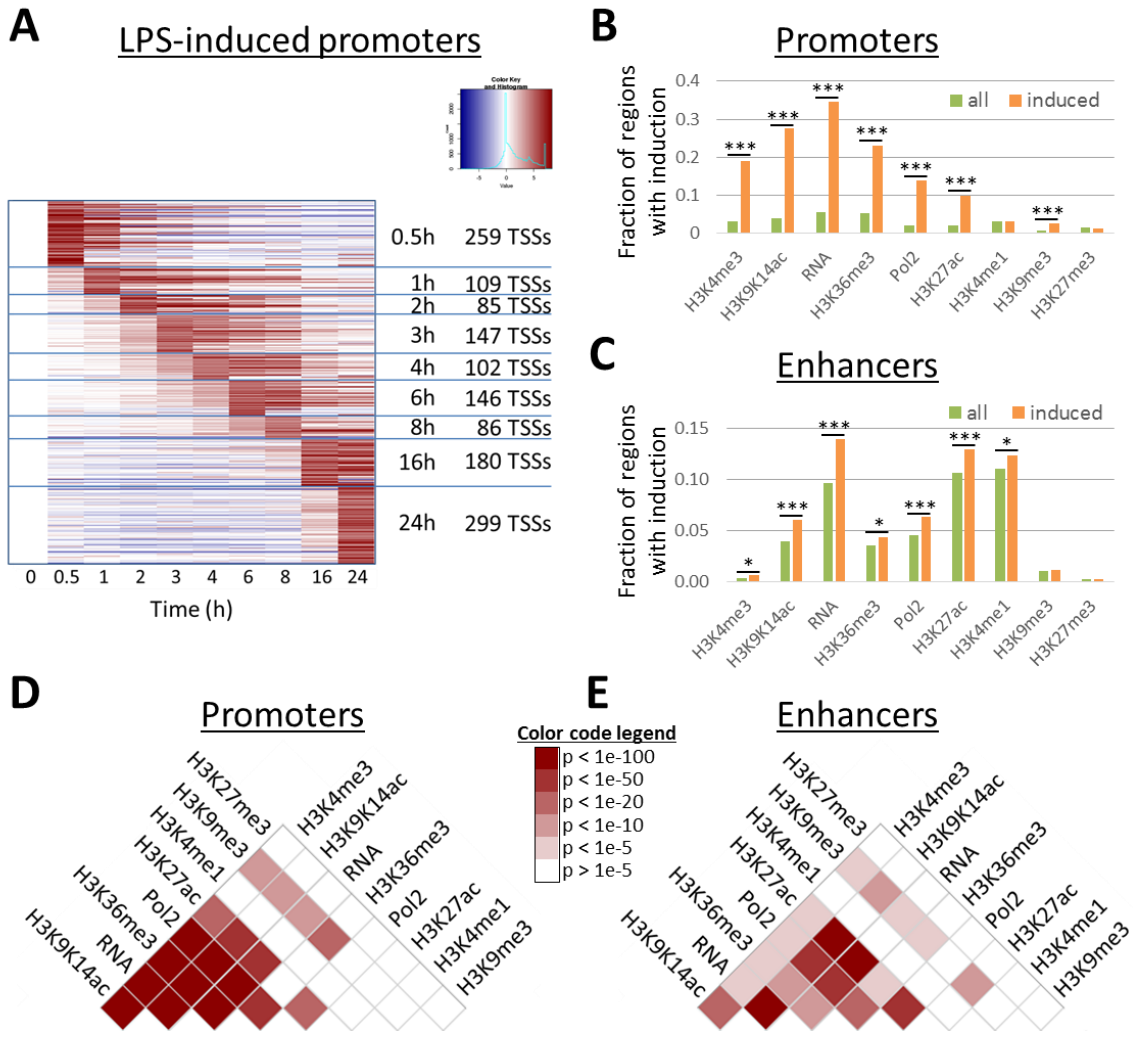

Fig. 1: *Frequencies of induction of features at LPS-induced promoters. (A) Heatmap showing the changes (white: no change; red: induction; blue: repression) in transcriptional activity of 1,413 LPS-induced promoters, relative to time point 0h. At the right, induction times and the number of promoters induced at each time point are indicated. (B) The fraction of promoters (y-axis) with increases in features (x-axis) are shown for the genome-wide set of promoters (green), and for the LPS-induced promoters (orange). Increases in H3K4me3, H3K9K14ac, H3K27ac, H3K36me3, RNA, and*

*Pol2 binding are observed relatively frequently at LPS-induced promoters. Significance of differences was estimated using Fisher's exact test; *: p < 1e-4; **: p < 1e-6; ***: p < 1e-10. (C) Same as (B), for enhancers. (D-E) Heatmaps indicating the overlap in induction of pairs of features. Colors represent p values (-log$_{10}$) of Fisher's exact test. White: low overlap; Red: high overlap. Plots are shown for promoters (D), and enhancers (E).*

Previous studies have reported only limited combinatorial complexity between histone modifications, i.e. subsets of modifications are highly correlated in their occurrence (Schübeler et al. 2004; Ernst et al. 2011). In our data too, basal levels of activation markers at promoters and, to a lesser degree at enhancers, were highly correlation (Fig. S3). Stimulus-induced accumulations of histone modifications and Pol2 binding at promoters and enhancers further support this view. For example, increases in H3K9K14ac, H3K4me3, H3K36me3, H3K27ac, Pol2 binding, and transcription often occurred at the same promoters (Fig. 1D). Similarly, increases in H3K9K14ac, H3K27ac, Pol2 binding, and transcription often coincided at enhancer regions (Fig. 1E). In general, activated regions experienced increases in several activation markers.

Several Histone Modifications are Induced at a Specific Time after Stimulation

Focusing on the set of induced promoters, we analyzed the ordering of induction times of different features (transcription activity, Pol2 binding, histone modifications). We defined the "induction time" of a feature *X* in a genomic locus as the first time point (if any) where *X* was increased significantly compared to its basal level in that loci (i.e. at 0h; see Methods). Defining induction times in individual genomic loci is not straightforward, due to the noisy nature of biological data. Therefore, we here focused on genome-wide trends by analyzing induction times in sets of promoters and enhancers.

As a proof of concept and a positive control, we observed that RNA reads (based on RNA-seq) mapped to promoter regions were generally induced at the same time and in the same order of the

induction of transcription initiation (based on TSS-seq, independent of RNA-seq data; Fig. 2A (top) and Fig. S4). E.g. at promoters with early induction of transcription initiation (TSS-seq) there was an early induction of mapped RNA reads, while those with later induction have later induction of mapped RNA reads. Plotting the same data using cumulative plots, we again observed that increases in RNA-seq reads roughly follow the same order as transcription induction times (Fig. 2A, bottom). Promoters of stably expressed genes lack induction of mapped RNA reads at their promoter. Similar observations were made for induction of Pol2 binding (Fig. 2B).

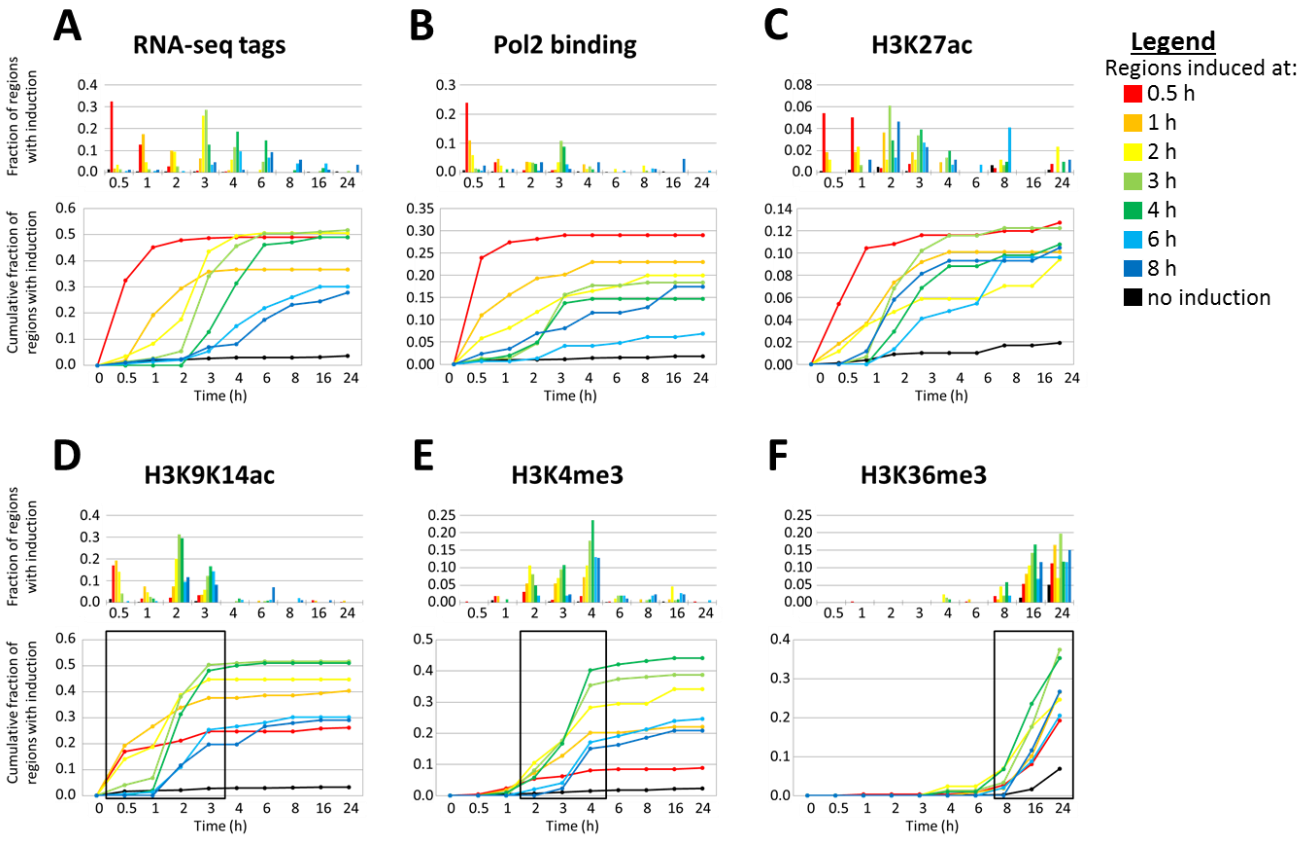

Fig. 2: *Induction times of transcription, Pol2 binding and histone modifications at promoters in function of induction of transcriptional activation times. (A-F) The fraction (top) and cumulative fraction (bottom) of promoters with an induction in RNA-seq reads (A), Pol2 binding (B), H3K9K14ac (C), H3K4me3 (D), H3K36me3 (E), and H3K27ac (F) are shown. Line colors represent promoters with different transcriptional activation times. Black boxes indicate time frames with frequent induction of a feature.*

However, in striking contrast, induction times of H3K9K14ac, H3K4me3, and H3K36me3 at LPS-induced promoters were concentrated within specific time windows (Fig. 2D-F), and, moreover, the time of induction of these markers appeared to be largely independent of transcriptional induction times. Induction of H3K9K14ac was in general concentrated between 0.5h and 3h after stimulation (Fig. 2D), although promoters with early induction of transcription (0.5h, 1h, 2h) tended to have early increases in H3K9K14ac (at 0.5h). Even genes with transcriptional induction at 3, 4h (and to a lesser extend 6 and 8h) had induction of H3K9K14ac mostly before 3h after stimulation. Therefore, the induction of acetylation for these promoters *preceded* induction of transcription. Very few promoters showed significant increases later than 3 hours after stimulation. Finally, at promoters with late induction (16h, 24h) or at stably active promoters, increases in H3K9K14ac were rare (not shown in Fig. 2 in the interest of clarity).

In contrast with H3K9K14ac, no significant induction of H3K4me3 was observed at time points 0.5h and 1h (Fig. 2E). Induction of H3K4me3 at LPS-induced promoters was concentrated between 2 and 4 hours after stimulation, regardless of their transcriptional induction times. While induction of H3K4me3 was rare at immediate-early promoters, between 20 to 45% of promoters induced at 1h, 2h, 3h, 4h, 6h, and 8h had significant increases of this modification. These results suggest that stimulus-induced accumulation of H3K4me3 is not necessarily a prerequisite nor a direct consequence of transcription induction, since it can both *precede* or *follow* induction of transcription (see also Discussion).

Finally, H3K36me3 was only induced at later time points, especially at 16h and 24h, regardless of transcriptional induction times of promoters (Fig. 2F). In contrast with H3K9K14ac and H3K4me3, H3K36me3 is located within gene bodies and peaks towards their 3' end (Fig. S5) (Barski et al. 2007). Upon stimulation, H3K36me3 gradually accumulated within the gene bodies of LPS-induced genes, spreading towards the 5' end, and reached the promoter region at the later time points in our time

series (Fig. S5A). Stably expressed genes had on average high basal levels of H3K36me3, with only limited changes over time. However, interestingly, at time points 16-24h, an accumulation of H3K36me3 was observed towards their 5' end (Fig. S5B), resulting in a relatively high fraction of stably expressed promoters having an induction of H3K36me3 (6.9%), whereas these promoters tended to lack induction of other modifications. Induction of H3K9me3 was rare at promoters, but this too had a tendency to occur at later time points (16h and 24h; Fig. S6A).

Remarkably, the induction times of H3K9K14ac, H3K4me3, and H3K36me3 at promoters did not change depending on their basal levels (Fig. S7); regardless of their pre-stimulus levels, increases in H3K9K14ac were early, followed by H3K4me3, and H3K36me3 accumulation was late. This might indicate that a common mechanism is regulating these accumulations, regardless of basal levels.

The tendencies described above were confirmed using RT-qPCR and ChIP-qPCR measuring RNA, H3K9K14ac, H3K4me3 (see WT data in Fig. 7), and H3K36me3 (Fig. S8) at the promoters of 9 LPS-induced genes. In general, accumulation of H3K9K14ac in WT occurred before that of H3K4me3, and accumulation of H3K36me3 was late.

Significant increases in H3K27ac appeared to be relatively rare at promoters (Fig. 2C), and were somewhat enriched at earlier time points (0.5h, 1h, and 2h). However, promoters with later induction of transcription experience later increases in H3K27ac. The pattern for H3K27ac therefore appeared to be an intermediate between that of H3K9K14ac (early increases), and that of RNA or Pol2 (increases follow transcription induction times). Very few inductions were observed for H3K27me3 and H3K4me1 (Fig. S6B-C).

Increases in histone modifications were more frequent at non-CpG promoters than at CpG island-associated promoters (Fig. S9). This can be explained by the lower basal levels of most activation-associated histone modifications at non-CpG promoters (Fig. S2B). However, regarding the timing of induction of modifications, no differences were observed between both types of promoters.

Similarities and Differences between Enhancer and Promoter Induction Patterns

Interactions between enhancers and promoters could allow histone modifiers active at promoters to also affect modifications at enhancer regions, and vice versa. We therefore analyzed induction of features at enhancers in function of the timing of induction of transcription at the promoter.

To some degree, we found similar tendencies at enhancers assigned to induced promoters. We found that a small fraction of RNA-seq reads was aligned to enhancers, indicating that polyA-tailed enhancer-associated transcripts were transcribed from these regions. Induction of enhancer-associated transcripts to some extent followed the order of transcription induction at nearby promoters, though they seemed to somewhat precede transcription induction at promoters, and increases were relatively frequent at early time points (0.5 and 1h; Fig. 3A). These observations fit with those reported in a recent study, showing that transcription at enhancers precedes that of promoters in cells treated with various stimuli (Arner et al. 2015). We observed a somewhat similar, though weaker, pattern for Pol2 binding at enhancers (Fig. 3B).

For H3K9K14ac, the induction pattern at enhancers was similar to that observed for promoters (Fig. 3C); induction of H3K9K14ac was mainly concentrated at time points 2h and 3h after stimulation. Although in general a lower percentage of enhancers experienced increases of H3K9K14ac than promoters (5-10% vs 20-50%), typically 20-40% of induced promoters had at least one assigned enhancer at which an induction of H3K9K14ac occurred (Fig. S10). Increases in H3K27ac at enhancers appeared to follow to some degree the order of transcription induction of nearby promoters (Fig. 3D), in a pattern that was more similar to that of Pol2 and RNA-seq reads.

Finally, for other modifications, there are discrepancies between promoters and enhancers. We observed a gradual increase in H3K4me1 markers at enhancers over the time course (Fig. S11A), and limited increases in H3K36me3 (Fig. S11B), again independent of timing of transcriptional induction. H3K4me3, H3K9me3, and H3K27me3 signals were in general low, and no increases were observed (Fig. S11C-E).

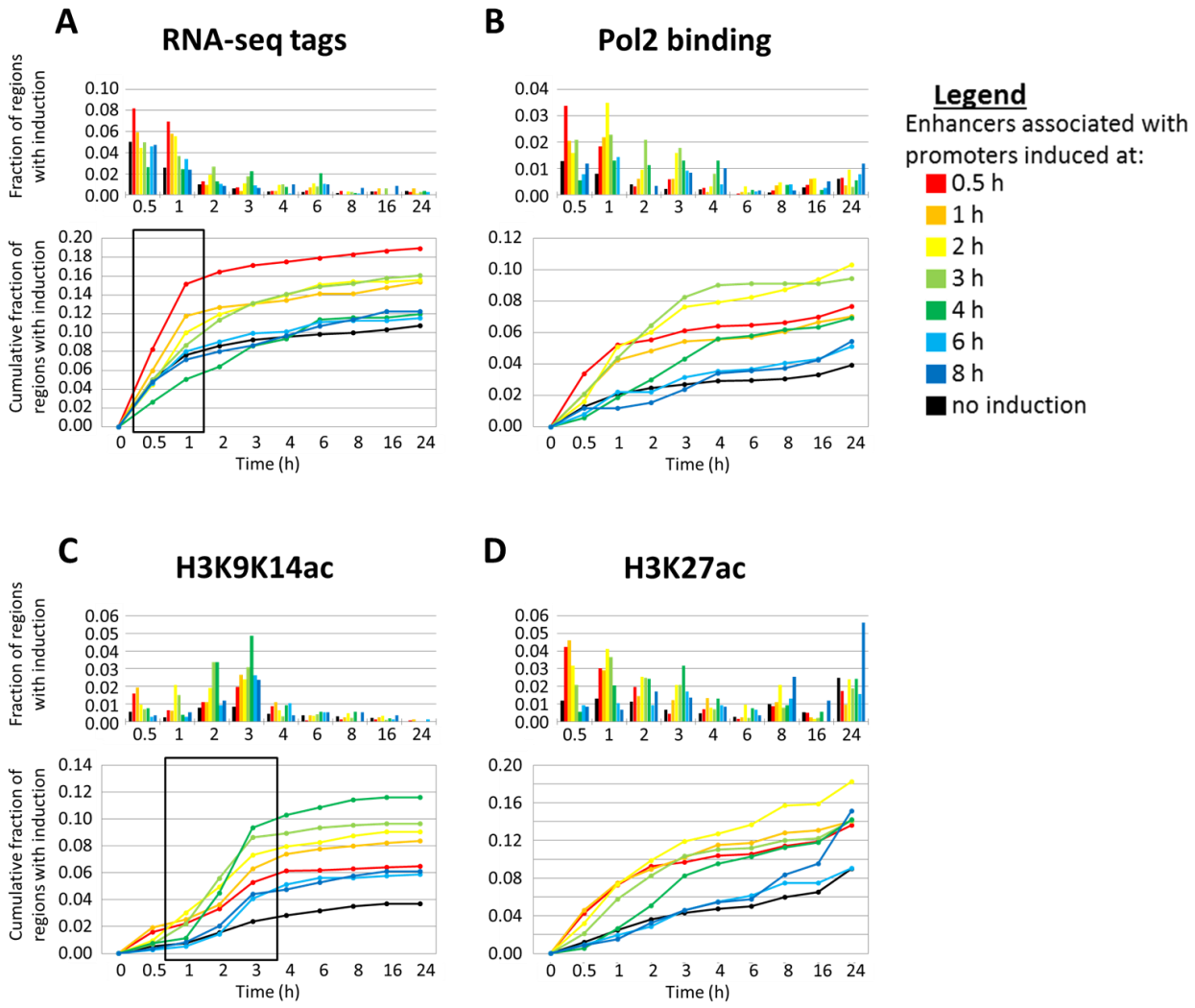

Fig. 3: *Induction times of RNA-seq reads (A), Pol2 binding (B), H3K9K14ac (C), and H3K27ac (D) at enhancers of LPS-induced promoters. Plots are similar to those shown in Fig. 2.*

Correlation between LPS-induced TF binding and increases in epigenetic features

Next, to reveal potential regulatory mechanisms underlying the epigenetic changes induced by LPS, we performed an integrative analysis of our histone modification data with TF binding data. For this we used a publicly available ChIP-seq dataset for 24 TFs with high expression in mouse DCs (Garber et al. 2012), before and after treatment with LPS (typical time points include 0h, 0.5h, 1h, and 2h, see Methods).

As reported in the original study, we observed widespread pre-stimulation binding of both stably-expressed and LPS-induced promoters by PU.1 and C/EBPβ, and to a lesser degree by IRF4, JUNB, and ATF3 (Garber et al. 2012) (Fig. S12A). The known association between H3K4me1 and binding by PU.1 and C/EBPβ was also successfully recapitulated (Fig. S13A,B) (Heinz et al. 2010; Ghisletti et al. 2010). Binding by TFs controlling the response to LPS, such as NF-κB (subunits NFKB1, REL, and RELA) and STAT family members, was relatively frequent at LPS-induced promoters (Fig. S12B).

Focusing on the overlap between LPS-induced TF binding at promoters and enhancers, and induction of epigenetic features, we found that new binding of promoters by RelA, IRF1, STAT1, and STAT2 was especially associated with increases in H3K9K14ac, H3K4me3, H3K36me3, transcription, and to a lesser degree Pol2 binding and H3K27ac (Fig. 4; Fisher's exact test). For example, of the 418 promoter regions that become newly bound by STAT1 after stimulation, 223 (53.3%) experience increases in H3K9K14ac (vs 3.0% of promoters not bound by STAT1; p: 8.3E-205). LPS-induced binding by the same four TFs was also strongly associated with increases in H3K9K14ac and H3K27ac at enhancers (Fig. 4). Combinations of these four TFs often bind to the same promoter and enhancer regions (Fig. S12C,D), and STAT1 functions both as a homodimer or as a heterodimer with STAT2 (Ramana et al. 2000). LPS-induced TFs, including NF-κB and STAT family members, have been shown to bind preferentially at loci that are pre-bound by PU.1, C/EBPβ, IRF4, JUNB, and ATF3 (Garber et al. 2012). Accordingly, histone modifications were also more frequently observed at regions that were pre-bound by these five TFs (Fig. S14).

Weaker associations were found for LPS-induced binding by other NF-κB subunits (NFKB1, REL, and RELB), TFs that are widely active even before stimulation (C/EBPβ, ATF3, JUNB, and IRF4), and E2F1, which has been shown to be recruited by NF-κB through interaction with Rela (Lim et al. 2007).

Together, these results suggests a strong correlation between increases in activation marker histone modifications and LPS-induced binding by RelA, IRF1, STAT1 and STAT2.

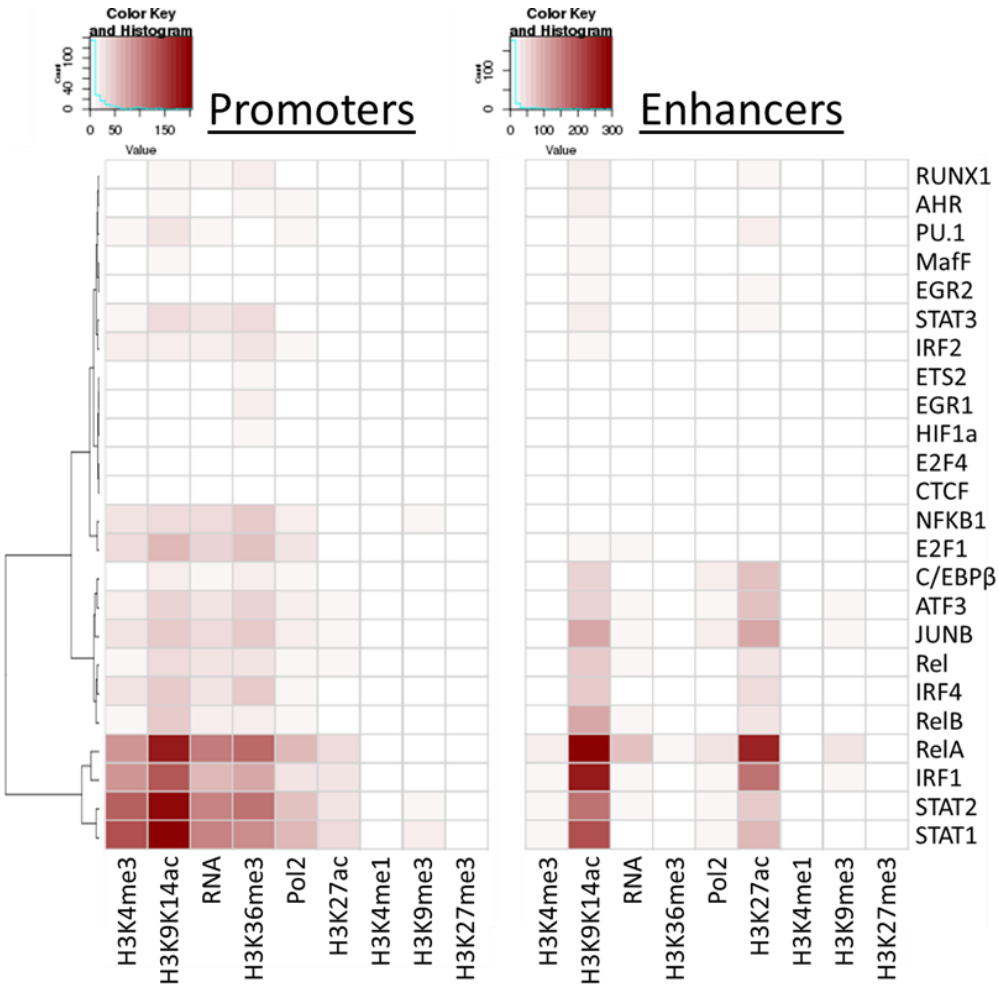

Fig. 4: *Associations between LPS-induced TF binding at promoters (left) and enhancers (right) and increases in histone modifications, Pol2 binding and transcription at the newly bound regions. Colors in the heatmap represent the degree of co-incidence (Fisher's exact test, -log$_{10}$ p values) between new TF binding events (rows) and increases (columns). TFs (rows) have been grouped through hierarchical clustering by similarity of their association pattern.*

STAT1 and STAT2 binding coincides with Increases in H3K9K14ac, and precedes Increases in H3K4me3

The relative timing of LPS-induced TF binding events and increases in histone modifications can reflect potential causal relationships in the above correlations. As described above, H3K9K14ac levels increase mainly during the first 3 hours after LPS stimulation (Fig. 2D). Particularly, many LPS-induced promoters show increases in H3K9K14ac between 2 and 3 hours after stimulation, and we

found a strong overlap between increases in H3K9K14ac and binding by STAT1 (Fig. 4). STAT1 is not active before stimulation, and its activity is only induced about 2 hours after LPS stimulation (Toshchakov et al. 2002), resulting in a strong increase in STAT1-bound loci (from 56 STAT1-bound loci at 0h to 1,740 loci at 2h; Fig. S12B).

We observed a particularly strong coincidence in timing between STAT1 binding and increases in H3K9K14ac (Fig. 5A): genomic regions that become bound by STAT1 at 2h show a coinciding sharp increase in H3K9K14ac around the STAT1 binding sites. Induction of H3K9K14ac was particularly frequent at promoters and enhancers that became bound by STAT1 at 2h (Fig. 5B,C). Very few promoters and enhancers that become bound by STAT1 at 2h have significant increases in H3K9K14ac at earlier time points. At the 2 hour time point, STAT1 binds 378 enhancers and 409 promoters, and at the same time there is a widespread induction of H3K9K14ac at these target regions (Fig. 5B,C). At the end of our time series, 222 (54.2%) of these promoters, and 214 (56.6%) of these enhancers, had significantly increased H3K9K14ac levels (versus only 3.0% of promoters and 3.3% of enhancers lacking STAT1 binding).

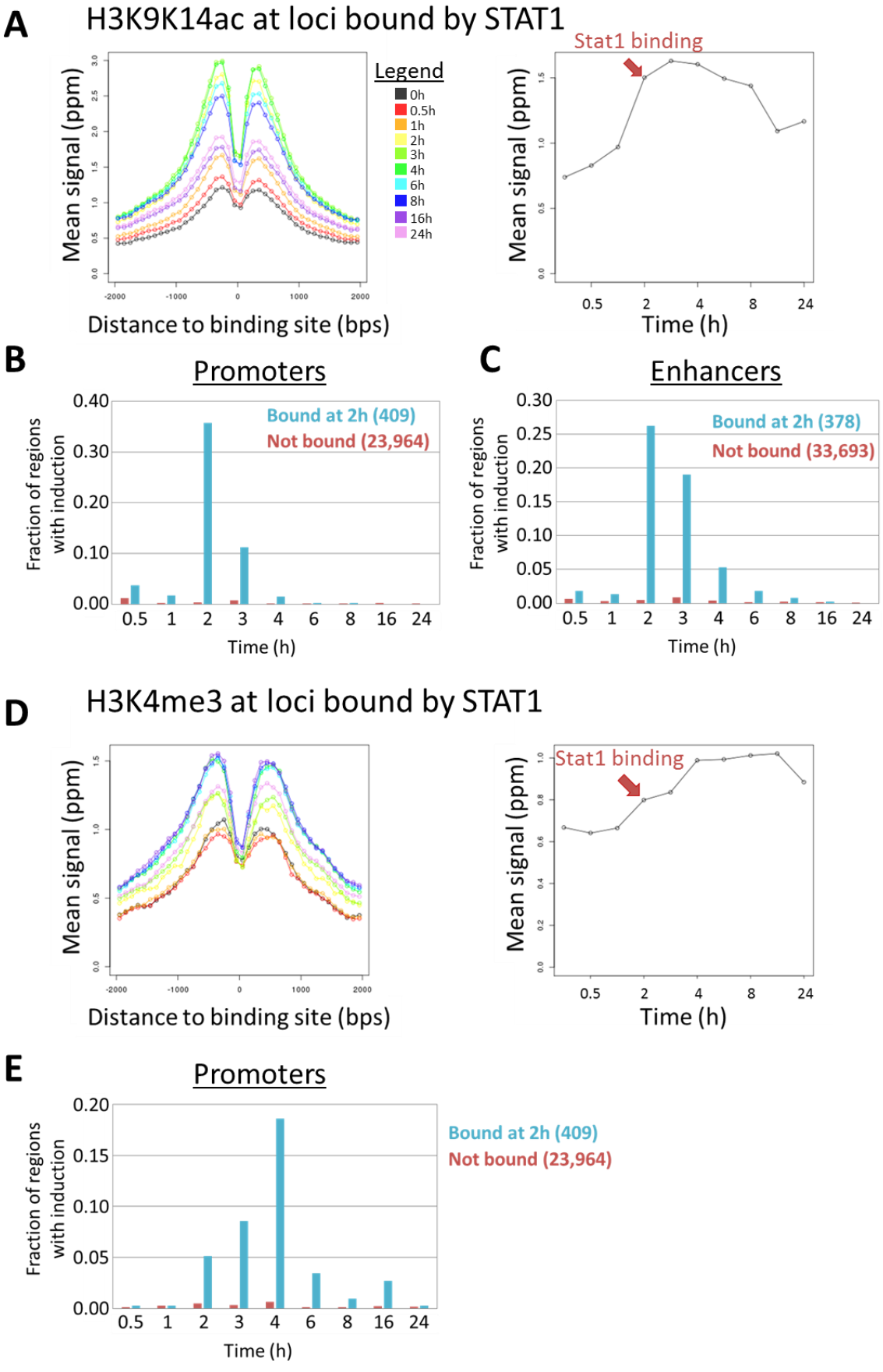

(Figure legend on next page)

Fig. 5: *Interaction between STAT1 binding and histone modifications. (A) For all genomic regions bound by STAT1 at 2h after LPS stimulation, mean H3K9K14ac signals are shown over time. Left: profile of mean values (y axis) over time in bins of 100 bps in function of distance (x axis) to the TF binding site. Right: mean values (y axis) summed over the region -2kb to +2kb over all bound regions, over time (x axis). The red arrow indicates the time at which these regions become bound by STAT1. (B) The fraction of promoters with induction of H3K9K14ac over time after stimulation (x axis). Blue: regions bound by STAT1 at time 2h. Red: regions not bound by STAT1 at any time point. Numbers in parentheses show the number of regions bound and not bound by STAT1 (C) As in (B) for enhancer regions bound (and not bound) by STAT1. (D) As in (A), for H3K4me3 at the genomic regions bound by STAT1 2 hours after LPS stimulation. (E) As in (B), for promoter regions with induction in H3K4me3.*

Similar to H3K9K14ac, we observed a general increase in H3K4me3 around STAT1 binding sites (Fig. 5D). However, in contrast with H3K9K14ac, STAT1 binding immediately precedes the induction of H3K4me3 (between 2-4 hours). Accordingly, only 21 STAT1-bound promoters (out of 409; 5.6%) had significant increases at 2 h, but an additional 111 promoters (27.1%) experienced increases at the following time points (3-4 hours; Fig. 5E). As noted above, H3K4me3 was in general absent at enhancers.

Similar patterns were observed for enhancers and promoters bound by STAT2 2 hours after stimulation (Fig. S15). In contrast, regions bound by RelA and IRF1 showed increased levels of H3K27ac and to a lesser degree H3K9K14ac at earlier time points (Fig. S16 and S17). Associations with H3K9K14ac induction after 2 hours were weak compared to STAT1/2. Average increases in H3K4me3 at RelA- and IRF1-bound regions were only modest (Fig. S16G-I and S17G-I), suggesting that the association between RelA- and IRF1-binding and H3K4me3 as seen in Fig. 4 is mostly through co-binding at STAT1/2-bound regions. Associations between histone modifications and binding by other TFs were in general weak (not shown; see also Fig. 4). No changes were observed in

H3K4me1 at STAT1/2-bound regions (Fig. S18A). Although there was a tendency for STAT1/2-bound loci to have increases in H3K27ac, binding seemed to slightly lag behind H3K27ac induction (Fig. S18B). Finally, although STAT1/2-bound regions tended to experience increases in H3K36me3, the time lag between binding and induction was large (Fig. S18C). This is also true for other TFs, such as RelA and IRF1, and even PU.1 and C/EBPβ, regardless of the timing of TF binding (Fig. S13C-F).

These results suggest possible causal relationships between TF binding events and induction of activation-associated histone modifications, especially between STAT1/2 binding and the accumulation of H3K9K14ac and H3K4me3. The specific timing of increases in these modifications possibly reflects the timing of activation of these TFs, resulting in the recruitment of acetyl transferases and methyl transferases to specific promoter and enhancer regions.

LPS-induced Accumulation of H3K9K14ac and H3K4me3 is especially frequent at STAT1/2-bound Promoters of TRIF-dependent Genes

In *Trif*$^{-/-}$ cells, LPS-induced type I IFN production, activation of the JAK-STAT pathway, and induction of STAT1 and STAT2 target genes are severely impaired. Under the hypothesis that there is a causal relation between STAT1/2 binding and induction of H3K9K14ac and/or H3K4me3, we would therefore expect an especially high overlap between genes with decreased expression in *Trif*$^{-/-}$ cells, and promoters with induction of H3K9K14ac or H3K4me3 following stimulation in the WT. On the other hand, MyD88-dependent but TRIF-independent genes should mostly lack STAT1 and STAT2 binding, and are therefore expected to lack induction of these modifications.

Using RNA-seq data from LPS-stimulated *Myd88*$^{-/-}$ and *Trif*$^{-/-}$ cells, we defined a set of 141 TRIF-dependent genes (Fig. 6A). These genes typically have induction around 3-6 hours after stimulation in WT and *Myd88*$^{-/-}$, but lack induction of transcription in the *Trif*$^{-/-}$ cells. We found that a high fraction of the TRIF-dependent genes were bound by STAT1 and STAT2 in the WT ChIP-seq samples 2 hours after stimulation (STAT1: 64.5%, STAT2: 57.4%; compare: MyD88-dependent genes: 10.6% and

9.1%; Fig. 6B). This suggests that these genes are indeed under the control of STAT1 and/or STAT2 in WT.

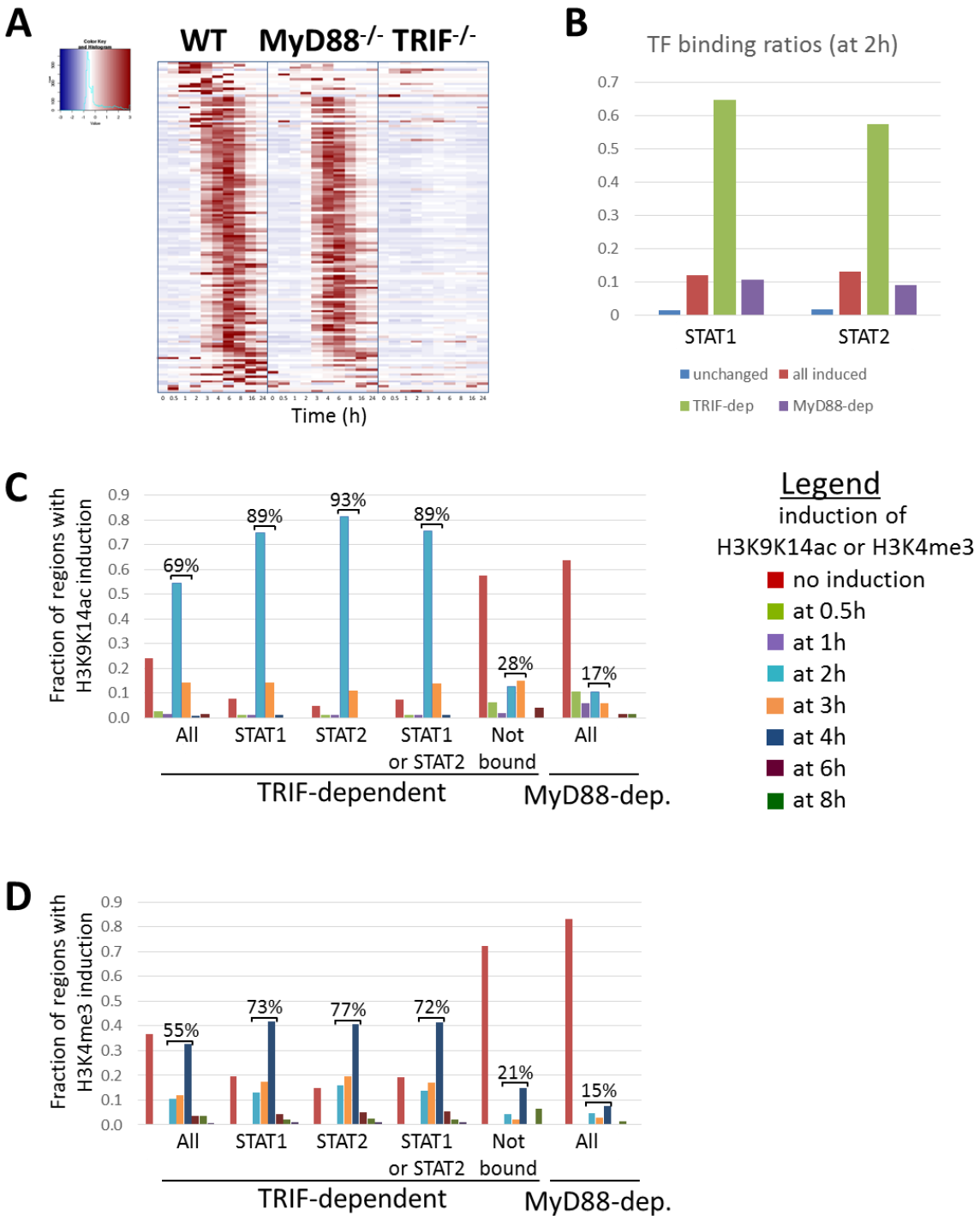

(Figure legend on next page)

Fig. 6: *Increase of H3K9K14ac and H3K4me3 at STAT1/2-bound promoters of TRIF-dependent genes. (A) Heatmap showing gene expression changes in WT,* Myd88$^{-/-}$*, and* Trif$^{-/-}$ *mice after LPS stimulation of mouse DCs for TRIF-dependent genes. (B) TF binding ratios of promoter regions with stable expression ("unchanged", blue), all LPS-induced promoters in WT (red), TRIF-dependent promoters (green), and MyD88-dependent promoters (purple). TRIF-dependent promoters are often bound by STAT1 and/or STAT2. (C) Fraction of regions with induction of H3K9K14 for TRIF- and MyD88-dependent promoters. For TRIF-dependent genes, plots are also shown specifically for STAT1 and/or STAT2 bound and unbound regions. Colors of bars indicate the timing of H3K9K14ac induction. (D) Same as (C) for H3K4me3 induction. Induction of H3K9K14ac and H3K4me3 is highly specific for STAT1/2 bound TRIF-dependent genes, and concentrated at time points 2-3 h and 2-4 h, respectively. Percentages indicate the fraction of regions with induction between 2-3 hours for H3K9K14ac, and between 2-4 hours for H3K4me3.*

Within these 141 TRIF-dependent genes, 97 (68.8%) had increases in H3K9K14ac at time points 2-3 hours (Fig. 6C). After dividing these TRIF-dependent genes by presence or absence of STAT1/2 binding, a clear difference in H3K9K14ac induction was observed: 81 out of 91 (89.0%) TRIF-dependent STAT1-bound genes, and 75 out of 81 (92.6%) of TRIF-dependent STAT2-bound genes had induction of H3K9K14ac between 2-3 hours. In contrast, only 13 out of 47 (27.7%) of TRIF-dependent genes lacking binding by STAT1 and STAT2 had induction of H3K9K14ac. As a reference, only 11 out of 66 (16.7%) of MyD88-dependent genes had H3K9K14ac induction at these time points.

A similar tendency was observed for H3K4me3 induction at time points 2-4h (Fig. 6D). 78 (55.3%) of TRIF-dependent genes had increases in H3K4me3 at time points 2-4 hours. Only 10 out of 47 (21.3%) TRIF-dependent genes lacking STAT1 and STAT2 binding, and only 10 out of 66 (15.2%) MyD88-

dependent genes had induction of H3K4me3 at these time points. In contrast, 66 (72.5%) of STAT1-bound, and 62 (76.5%) of STAT2-bound promoters had increases.

A Subset of STAT1/2 Target Genes lack Induction of H3K9K14ac and H3K4me3 in *Trif*$^{-/-}$, *Irf3*$^{-/-}$, and *Ifnar1*$^{-/-}$ cells

We further analyzed the roles of the TRIF-dependent signaling pathway and STAT1/2 in regulating LPS-induced genes, using RT-qPCR and ChIP-qPCR in WT, *Trif*$^{-/-}$, *Irf3*$^{-/-}$, and *Ifnar1*$^{-/-}$ cells. Experiments were performed on a selection of known TRIF-dependent and TRIF-independent genes, which showed increases in H3K9K14ac and H3K4me3 in WT (Fig. 7).

A set of known TRIF-independent genes (*Tnf*, *Il1b*, *Cxcl1*, and *Nfkbiz*) had no change between WT and knock outs (KOs) in the induction of gene expression, H3K9K14ac and H3K4me3 (Fig. 7A). These genes are not bound by STAT1/2 (except for *Cxcl1* which is bound only by STAT2), and we can assume that the induction of histone modifications at their promoter regions is STAT1/2-independent.

A second subset of LPS-induced genes (*Ifit1* and *Rsad2*) has TRIF-dependent expression. These genes become bound by STAT1/2 2 hours after LPS stimulation. Their expression and the induction of H3K9K14ac and H3K4me3 were completely abrogated in *Trif*$^{-/-}$ cells, in *Irf3*$^{-/-}$ cells, and in *Ifnar1*$^{-/-}$ cells (Fig. 7B). These results further support a role of STAT1 and/or STAT2 in the control of chromatin modifications at the promoters of these genes.

A third subset of genes (*Cxcl10*, *Ccl5*, and *Il6*) was partially dependent on TRIF, IRF3, and IFNR in their induction of gene expression and histone modification changes (Fig. 7C). Induction of H3K4me3 was abrogated for *Cxcl10* in all three KOs, although H3K9K14ac was only affected in *Trif*$^{-/-}$cells. Modifications at *Ccl5* and *Il6* too, showed a dependency of TRIF, but not on IFNR. Although these three genes were bound by STAT1 or STAT2 2 hours after LPS stimulation, it is likely that their gene expression and histone modifications are regulated by additional, partly redundant signaling

pathways downstream of TLR4 (Hirotani et al. 2005). Indeed, RelA and IRF1 bind to the promoters of these genes, supporting the notion of combinatorial control of gene expression and histone modifications.

Furthermore, stimulation of WT cells using IFN-β induced expression of *Ifit1* and *Rsad2*, and accumulation of H3K9K14ac and H3K4me3 at their promoters (Fig. S19B). In this system, the activation of the IFNR signaling pathway, and of STAT1/2, is independent of TRIF. Accordingly, this accumulation of H3K9K14ac and H3K4me3 was not affected in *Trif*$^{-/-}$ cells, further supporting a role for STAT1/2 in the control of these modifications at these genes. Similar accumulations were observed for *Cxcl10*, *Ccl5*, and *Il6* (Fig. S19C). Although the resolution of the data is not enough to make a definite statement, accumulation of H3K9K14ac following IFN-β stimulation had a tendency to start earlier at several of these five promoters in both WT and *Trif*$^{-/-}$ cells, compared to LPS-stimulated cells, possibly reflecting a faster activation of STAT1/2. In contrast, no or only limited accumulation was not observed for *Tnf*, *Il1b*, *Cxcl1*, and *Nfkbiz* (Fig. S19A).

Fig. 7: *Gene expression (mRNA), H3K9K14ac and H3K4me3 dynamics in WT,* Trif$^{-/-}$, Irf3$^{-/-}$, *and* Ifnar$^{-/-}$ *cells following LPS stimulation. We distinguished genes of which expression and histone modifications are independent (A), dependent (B), and partially dependent (C) on TRIF, IRF3, and IFNR. Error bars represent the standard deviation based on duplicate experiments. The red dotted line in each graph represents the mean value at 0h. Y axes represent fold induction (for mRNA) and % input (for H3K9K14ac and H3K4me3). Binding of promoters by RelA, IRF1, STAT1 and STAT2 is indicated at the right hand side (white: no binding, purple: binding by RelA, green: binding by IRF1, blue: binding by STAT1, red: binding by STAT2).*

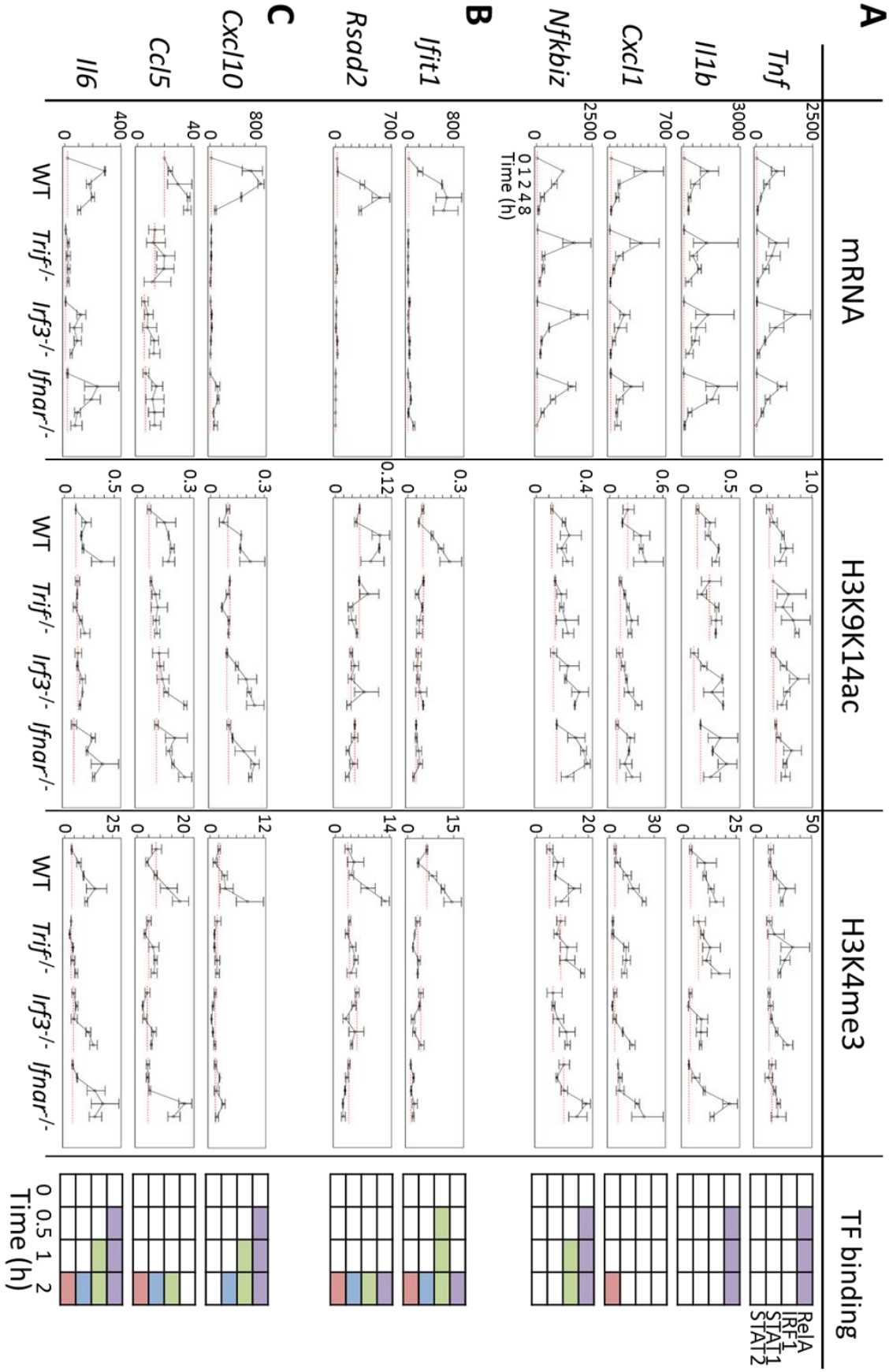

(Figure legend on previous page)

Discussion

The concept of active genes being in an open chromatin conformation was introduced several decades ago (Weintraub and Groudine 1976), yet the contribution of histone modifications to the control of gene activity remains controversial (Henikoff and Shilatifard 2011). On the other hand, the contribution of TFs to regulating gene expression is widely recognized (Lenhard et al. 2012), and a few studies have identified crosstalk between TFs and histone modifiers as important in the regulation of the response to immune stimuli. Induction of enhancer histone modifications was found to be associated with LPS stimulation-induced gene expression (Ostuni et al. 2013). IκBζ was shown to control gene expression of *Lcn2* and *Il12b* as well as H3K4me3 in their promoters (Kayama et al. 2008). This process further induces recruitment of the SWI/SNF chromatin remodeling complex, which is regulated by Akirin2 (Tartey et al. 2014). Histone modifications such as deacetylation by histone deacetylases (Chen et al. 2012) and H3K9me3 demethylation by Jmjd2d (Zhu et al. 2012), have been linked to the induction of a small set of genes upon LPS stimulation. Nevertheless, our understanding about causal relationships between TF binding, changes in histone modifications, and changes in transcriptional activity of genes in response to stimuli is still lacking.

Analysis of the ordering of events over time can reveal insights into possible causal relationships or independence between them. Here, we presented an integrative study of the timing and ordering of changes in histone modifications, in function of transcriptional induction in response to an immune stimulus. Our results suggest that rather than a clear temporal order between stimulus-induced chromatin remodeling followed by transcriptional activation, specific histone modifications appear to be induced at specific time frames after stimulation. These time frames appear to be relatively independent of the timing of induction of transcription.

In our dataset, we roughly observed three “waves” of modifications. The first was early induction of H3K9K14ac, which occurs mainly in the first three hours after stimulation. Here, we did observe that some immediate-early promoters tended to have immediate induction of acetylation. However,

changes were concentrated at time points 2h and 3h. A second wave consisted of H3K4me3, occurring mainly at 2-4 hours following stimulation. For genes with early transcriptional induction, this modification therefore only occurs *after* induction of transcription, while it *precedes* induction of transcription for genes with later induction times. Although H3K4me3 is widely used as a marker for active genes, the functional role of this modification is still unclear. For example, the deletion of Set1, the only H3K4 methyltrasferase in yeast, resulted in slower growth than in wild type, but otherwise appears to have only limited effects on transcription (Miller et al. 2001). Other studies too have reported a lack of a direct effect of H3K4me3 on transcription (Pavri et al. 2006; Stasevich et al. 2014). Another study showed that H3K4 methyltransferase Wbp7/MLL4 controls expression of only a small fraction of genes directly (Austenaa et al. 2012). Together, these and our results hint at a lack of a causal relationship between transcription and H3K4me3 on a genome-wide scale. Finally, a third and last wave consisted of changes in H3K36me3 and H3K9me3, occurring only around 16-24 hours after stimulation. On the other hand, induction of H3K27ac was not limited to a specific time frame, but was more correlated with transcription induction times. Interestingly, fluorescence microscopy experiments have shown that H3K27ac levels, and not H3K4me3, can alter Pol2 kinetics by up to 50% (Stasevich et al. 2014). The induction time patterns of histone modifications could therefore indeed present hints about active or passive roles of different histone modifications.

Since the induction of remodeling appears to occur specifically at LPS-induced genes, it is likely that histone modifiers are recruited by one or more LPS-activated TFs to specific target regions in the genome defined by the binding specificity of the TFs. In this scenario, the timing of activation of the TFs could explain the “waves” of histone modification changes. This fits well with our observations for STAT1/2 and the induction of H3K9K14ac and H3K4me3, within specific time frames and mostly restricted to LPS-induced promoters. Other studies have reported associations between STAT1 binding and changes in epigenetic markers following environmental stimulation, including the activation of latent enhancers (Ostuni et al. 2013) and histone acetylation (Chen et al. 2012; Vahedi et al. 2012). Moreover, epigenetic priming by histone acetylation through STAT1 binding to

promoters and enhancers of *Tnf*, *Il6*, and *Il12b* has been reported (Qiao et al. 2013). Interestingly, these genes lack canonical STAT1 binding sites, and the acetylation at these genes did not directly result in transcriptional induction, but enhanced TF and Pol2 recruitment after subsequent TLR4 activation. Since TFs such as STAT1 are also known to induce gene expression, one might expect induction of histone modifications to co-occur with induction of expression. However, as we described here, and as supported by the above studies, this is not necessarily the case. Gene expression is known to be regulated by combinations of TFs, and in this study too we noticed that LPS-activated TFs such as NF-κB, IRF1 and STATs often bound to the same loci (Fig. S12), which were moreover often pre-bound by several other TFs, including PU.1 and C/EBPβ. Discrepancies between timing of expression induction and induction of histone modifications could be caused by different requirements for combinatorial binding. This could explain widely-reported "non-functional" TF binding, where TF binding does not seem to affect the activity of nearby genes (MacQuarrie et al. 2011). Such "non-functional" TF binding might instead trigger changes in histone modifications that remain unnoticed and affect gene activity in more subtle ways.

Although many studies have compared histone modifications before and after stimulation, most lack sufficient time points and resolution to allow analysis of temporal ordering of changes. One recent study in yeast reported results that are partly similar to ours (Weiner et al. 2015): specific modifications (especially, but not only, acetylation) occur at earlier time frames during the response of yeast to diamide stress, and others at later time points. Interestingly, even late changes in histone modifications in yeast (including H3K36me3) were reported to occur within just one hour after stimulation. In contrast, changes in H3K36me3 in our data were concentrated between 16-24 hours after stimulation. Thus, the time scales of stimulus-induced epigenetic changes in multicellular, higher mammalian systems might be much longer. Interestingly, increases in H3K36me3 around 16-24 h often coincide with a decrease in histone acetylation towards pre-stimulation levels at LPS-induced promoters. A study in yeast suggested that H3K36me3 plays a role in the activation of a

histone deacetylase (Drouin et al. 2010), and might therefore play a role in the return to a basal state of histone modifications and terminating the response to stimulus.

Our data and analysis presents a first genome-wide view of the temporal order of chromatin changes during a stress response in a mammalian immune cell. Integrative analysis of histone modification data with complementary datasets, as done in our study, can be used not only for finding correlations between TF and Pol2 binding and histone modifications, but also for suggesting hypotheses regarding the way these different levels of regulation interact with each other.

Material and Methods

Reagents, cells, and mice

Bone marrow cells were prepared from C57BL/6 female mice, and were cultured in RPMI 1640 supplemented with 10 % of fetal bovine serum under the presence of murine granulocyte/monocyte colony stimulating factor (GM-CSF, purchased from Peprotech) at the concentration of 10 ng/mL. Floating cells were harvested as bone marrow derived dendritic cells (BM-DCs) after 6 days of culture with changing medium every 2 days. The cells were stimulated with LPS (Salmonella minnessota Re595, purchased from Sigma) at the concentration of 100 ng/mL for 0, 0.5, 1, 2, 3, 4, 6, 8, 16, and 24 hours, and were subjected to RNA extraction or fixation. Murine IFN-β was purchased from Pestka Biomedical Laboratories, and was used to stimulate the cells at the concentration of 1x10^2 unit/mL. All animal experiments were approved by the Animal Care and Use Committee of the Research Institute for Microbial Diseases, Osaka University, Japan (IFReC-AP-H26-0-1-0). TRIF-, IRF3-, or IFNR-deficient mice have been described previously (Yamamoto et al. 2003; Saitoh et al. 2011; Hemmi et al. 2003).

ChIP-seq experiments

For each time point, thirty million BM-DCs were stimulated with LPS and subjected to fixation with addition of 1/10 volume of fixation buffer (11% formaldehyde, 50 mM HEPES pH 7.3, 100 mM NaCl,

1 mM EDTA pH 8.0, 0.5 mM EGTA pH8.0). The cells were fixed for 10 minutes at room temperature, and immediately washed with PBS three times. ChIP and sequencing were performed as described (Kanai et al, DNA Res, 2011). Fifty microliter of lysate after sonication was aliquoted as "whole cell extract" (WCE) control for each IP sample. Antibodies used were Pol2 (05-623, Millipore), H3K4me3 (ab1012, Abcam), H3K9K14ac (06-599, Millipore), H3K36me3 (ab9050, Abcam), H3K9me3 (ab8898, Abcam), H3K27me3 (07-449, Milllipore), H3K4me1 (ab8895, Abcam), and H3K27ac (ab4729, Abcam).

RNA extraction and RT-qPCR.

One million BM-DCs were stimulated with LPS for indicated times and subjected to RNA extraction by using TRIzol (Invitrogen) according to manufacturer's instruction. RNAs were reverse transcribed by using RevaTra Ace (Toyobo). The resulting cDNAs were used for qPCR by using Thunderbird SYBR master mix (Toyobo) and custom primer sets (Table S1). QPCR was performed by using LightCycler Nano (Roche).

ChIP-qPCR

ChIP was done as above, except 4x10^6 cells were used. The resulting ChIP-DNAs were subjected to qPCR as same as RT-qPCR, using custom primer sets (Table S2).

Peak calling and processing of ChIP-seq data

For each histone modification and for Pol2 binding data, we aligned reads to the genome, conducted peak calling and further processing as follows.

We mapped sequenced reads of ChIP-seq IP and control (WCE) samples using Bowtie2 (version 2.0.2), using the parameter "very-sensitive", against the mm10 version of the mouse genome (Langmead and Salzberg 2012). Processing of alignment results, including filtering out low MAPQ alignments (MAPQ score < 30) was performed using samtools (Li et al. 2009).

We predicted peaks for each time point using MACS (version 1.4.2) (Feng et al. 2012), using each IP sample as input and its corresponding WCE sample as control. To improve the detection of both

narrow and broad peaks, peak calling was performed using default settings and also using the "nomodel" parameter with "shiftsize" set to 73. Negative control peaks were also predicted in the control sample using the IP sample as reference. Using the predicted peaks and negative control peaks, we set a threshold score corresponding to a false discovery rate (FDR) of 0.01 (number of negative control peaks vs true peaks), for each time point separately. All genomic regions with predicted peaks were collected over all 10 time points, and overlapping peak regions between time points were merged together. Moreover, we merged together peak regions separated by less than 500 bps. This gave us a collection of all genomic regions associated with a peak region in at least one sample of the time series.

In a next step, we counted the number of reads mapped to each region at each time point for both the IP samples and WCE control samples. Using these counts, we performed a read count correction, as described by Lee et al. (Lee et al. 2012). Briefly, this method subtracts from the number of IP sample reads aligned to each peak region the expected number of non-specific reads given the number of reads aligned to the region in the corresponding WCE sample. The resulting corrected read count is an estimate of the number of IP reads in a region that would remain if no WCE reads are present (Lee et al. 2012). This correction is necessary for the quantitative comparison of ChIP signals over time in the downstream analysis.

Finally, the corrected read counts were converted to reads per kilobase per million reads (RPKM) values (using read counts and the lengths of each region), and normalized using quantile normalization, under the assumption that their genome-wide distribution does not change substantially during each time series. The normalized RPKM values were converted to read per million read (ppm) values.

TSS-seq data processing and promoter definition

TSS-seq data for BM-DCs before and after stimulation with LPS was obtained from the study by Liang *et al*. (Liang et al. 2014) (DDBJ accession number DRA001234). TSS-seq data reflects transcriptional

activity, but also allows for the detection of TSSs on a genome-wide scale at a 1 base resolution (Tsuchihara et al. 2009). Mapping of TSS-seq samples was done using Bowtie2, as for ChIP-seq data. The location (5' base) of the alignment of TSS-seq reads to the genome indicates the nucleotide at which transcription was started. In many promoters, transcription is initiated preferably at one or a few bases. Because of this particular distribution of TSS-seq reads mapped to the genome, default peak calling approaches cannot be applied. Instead, we used the following scanning window approach for defining regions with significantly high number of aligned TSS-seq reads.

The number of TSS-seq reads mapped to the genome in windows of size 1, 10, 50, 100, 500, and 1000 bases were counted in a strand-specific way, in steps of 1, 1, 5, 10, 50, and 100 bases. As a control, a large number of sequences was randomly selected from the mouse genome, and mapped using the same strategy, until an identical number of alignments as in the true data was obtained. For these random regions too, the number of reads was counted using the same scanning window approach. The distribution of actual read counts and control read counts were used to define a FDR-based threshold (FDR: 0.001) for each window size. For overlapping regions with significantly high read counts, the region with the lowest associated FDR was retained.

In order to remove potentially noisy TSSs, we removed TSSs that were located within 3' UTRs, and TSSs located >50 kb upstream of any known gene. For remaining TSSs, we used a simple model (see Supplementary material) 1) to decide the representative TSS location in case a promoter region contained several candidate main TSSs, 2) to remove TSS-seq hits lacking typical features of promoters (e.g. presence of only TSS-seq reads in absence of histone modifications and Pol2 binding), and 3) to decide the main promoter of a gene in case there were multiple candidates. Finally, we obtained 9,964 remaining high-confidence TSSs, each assigned to 1 single Refseq gene.

These TSS-seq-based TSSs were supplemented with 14,453 non-overlapping Refseq-based TSSs for all Refseq genes which did not have an assigned high-confidence TSS-seq-based TSS. Most of the genes associated with these TSSs had lower expression in our RNA-seq data (mostly RPKM is 0 or < 1;

not shown). Together, TSS-seq-based TSSs and Refseq-based TSSs resulted in a total of 24,416 promoter regions.

CpG-associated promoters were defined as those having a predicted CpG island (from the UCSC Genome Browser Database) in the region -1kb to +1kb surrounding the TSS (Meyer et al. 2013). Other promoters were considered to be non-CpG promoters.

Definition of enhancers

Enhancers were defined based on the signals of H3K4me1 and H3K4me3. First, we collected all genomic regions with significantly high levels of H3K4me1 (see section "Peak calling and processing of ChIP-seq data") in at least one of the ten time points. Regions located proximally (<2kb distance) to promoter regions and exons were removed, because they are likely to be weak H3K4me1 peaks observed around promoters, as were H3K4me1-positive regions of excessively large size (>10kb). Finally, we removed regions with H3K4me1 < H3K4me3 * 5, resulting in 34,072 remaining enhancers.

Enhancers were naively assigned to the nearest promoter (TSS-seq based or Refseq-based) that was < 150kb separated from it (center-to-center). For 30,448 enhancers (89%) a promoter could be assigned.

Public ChIP-seq data for TFs

Genome-wide binding data (ChIP-seq) is available for mouse DCs before and after stimulation with LPS, for a set of 24 TFs with a known role of importance and/or high expression in DCs (Garber et al. 2012) (GEO accession number GSE36104). TFs (or TF subunits) included in this dataset are Ahr, ATF3, C/EBPβ, CTCF, E2F1, E2F4, EGR1, EGR2, ETS2, HIF1a, IRF1, IRF2, IRF4, JUNB, MafF, NFKB1, PU.1, Rel, RelA, RelB, RUNX1, STAT1, STAT2, and STAT3. Typically time points in this data are 0h, 0.5h, 1h, and 2h following LPS stimulation (some TFs lack one or more time points). We used the ChIP-seq-based peak scores and score threshold as provided by the original study as an indicator of significant TF binding.

Promoters (region -1kb to +1kb around TSS) and enhancers (entire enhancer region or region -1kb to +1kb around the enhancer center for enhancers < 2 kb in size) were considered to be bound by a TF if they overlapped a ChIP-seq peak with a significantly high peak score. New binding events by a TF at a region were defined as time points with a significantly high score where all previous time points lacked significant binding.

Definition of induction of histone modifications and Pol2 binding

In order to analyze induction times of increases in histone modifications and Pol2 binding, we defined the induction time of a feature as the first time point at which a significant increase was observed compared to its original basal levels (at 0h). Significant increases were defined using an approach similar to methods such as by DESeq and voom (Anders and Huber 2010; Law et al. 2014), which evaluate changes between samples taking into account the expected variance or dispersion in read counts in function of mean read counts. This approach is necessary because regions with low read counts typically experience high fold-changes because of statistical noise in the data. Here we slightly modified this approach to be applicable to our data (10 time points without replicates; ppm values per promoter/enhancer region).

The values of all histone modifications, Pol2, RNA-seq, TSS-seq reads (ppms, for each time point) were collected for all promoters (region -1kb to +1kb) and enhancers (entire enhancer region or region -1kb to +1kb around the enhancer center for enhancers < 2 kb in size). For each feature (all histone modifications and Pol2 binding), we calculated the median and standard deviation in ppm values for each region, over the 10 time points. Dispersion was defined as follow:

$$d_{x,f} = \left(\frac{s_{x,f}}{m_{x,f}}\right)^2 \quad [1]$$

where $d_{x,f}$, $s_{x,f}$, and $m_{x,f}$ represent the dispersion, standard deviation, and median of feature f in region x over the 10 time points of the time series. Fitting a second order polynomial function on the $\log(d_{x,f})$ as a function of $\log(m_{x,f})$ for all promoter and enhancer regions, we obtained expected

dispersion values in function of median ppm value (see for example Fig. S20 for H3K9K14ac). From fitted dispersion values, fitted standard deviation values $s_{x,f,fitted}$ were calculated (see Eq. [1]), and 0h-based Z-scores were calculated as follows:

$$Z_{x,f,t} = \frac{(ppm_{x,f,t} - ppm_{x,f,0h})}{s_{x,f,fitted}} \quad [2]$$

where $Z_{x,f,t}$ is the Z-score of feature f in region x at time point t, and $ppm_{x,f,t}$ is the ppm value of feature f in region x at time point t. The induction time of a feature f at region x was defined as the first time point where $Z_{x,f,t}$ ≥4. To further exclude low-signal regions we added this additional threshold: the region should have a ppm value ≥ the 25 percentile of non-0 values in at least 1 time point. If Z-scores did not exceed 4 at any time point, the feature was regarded as not induced at a region. We used a similar approach to define LPS-induced promoters using TSS-seq data (see below).

For the analysis of induction times of H3K9K14ac, H3K4me3, and H3K36me3 at enhancers in function of their pre-stimulation basal levels (Fig. S7), we divided promoters into three classes according to their basal levels of each modifications as follows: Promoters lacking a modifications altogether (0 tag reads after correction described above) were considered as one class (“absent”). The remaining promoters were sorted according to their basal level of the modification, and were divided into two classes (“low basal level”, and “high basal level”) containing the same number of promoters.

Definition of LPS-induced promoters, unchanged promoters

LPS-induced promoters were defined using TSS-seq ppm values. LPS-induced promoters should have $Z_{x,TSS-seq,t}$ ≥4 for at least 1 time point and have TSS-seq ppm ≥1 at at least 1 time point. Only TSS-seq reads aligned in the sense orientation were considered for this (e.g. they should fit the orientation of the associated gene). For each of the thus obtained 1,413 LPS-induced promoters, the transcription induction time was defined as the first time point for which $Z_{x,TSS-seq,t}$ ≥4 was observed. Unchanged promoters were defined as those promoters having absolute values of $Z_{x,TSS-seq,t}$ < 1 for all time points, leading to 772 promoters.

RNA-seq data processing for wild type, *Trif*$^{-/-}$ and *Myd88*$^{-/-}$ cells

RNA-seq data for bone mouse BM-DCs treated with LPS were obtained from a the study by Patil *et al.* (Patil et al. 2013) (SRA accession number DRA001131). This data includes time series data for WT, as well as *Trif*$^{-/-}$ mice and *Myd88*$^{-/-}$ mice.

Mapping of RNA-seq data was performed using TopHat (version 2.0.6) and Bowtie2 (version 2.0.2) (Kim et al. 2013; Langmead and Salzberg 2012). Mapped reads were converted to RPKM values (Mortazavi et al. 2008) using gene annotation data provided by TopHat. RNA-seq data obtained from the *Myd88*$^{-/-}$ and *Trif*$^{-/-}$ mice was processed in the same way. RPKM values were subjected to quantile normalization over all 10 time points.

For genes corresponding to the LPS-induced promoters, the maximum fold-induction was calculated in the WT RNA-seq data. The same was done in the *Trif*$^{-/-}$ RNA-seq data, and in the *Myd88*$^{-/-}$ RNA-seq data. TRIF-dependent genes were defined as genes for which the fold-induction was more than 5 times lower in the *Trif*$^{-/-}$ data than in WT, leading to 141 TRIF-dependent genes (see Fig. 6A). Similarly, 66 MyD88-dependent genes (not shown) were defined as having more than 5 times lower induction in the *Myd88*$^{-/-}$ than in WT.

Fisher's exact test

We used Fisher's exact test to evaluate the significance of differences between induced and non-induced promoters and enhancers (Fig. 1A,B), the significance of associations between changes of pairs of features (Fig. 1C,D), and the association between TF binding and increases in histone modifications, Pol2 binding and transcription (Fig. 4 and Fig. S14).

Data Access

ChIP-seq data for Pol2, H3K4me3, H3K9K14ac, H3K36me3, H3K9me3, H3K27me3, H3K4me1, and H3K27ac are available from DDBJ, accession number DRA004881.

Acknowledgements

We thank the members of the Immunology Frontier Research Center (IFReC) Immuno-Genomics Research Unit and the Quantitative Immunology Research Unit for helpful discussions and advice, A. Yoshimura, E. Kurumatani, Y. Kimura, A. Yamashita, K. Imamura, K. Abe and T. Horiuchi for technical assistance and M. Ogawa for secretarial assistance. Computational time was provided by the computer cluster of the IFReC Laboratory of Systems Immunology. This work was supported by the Japan Society for the Promotion of Science (JSPS) through the "Funding Program for World-Leading Innovative R&D on Science and Technology (FIRST Program)", initiated by the Council for Science and Technology Policy (CSTP), and by a Kakenhi Grant-in-Aid for Scientific Research (JP23710234) from the Japan Society for the Promotion of Science.

Disclosure Declaration

The authors declare no conflicts of interest.

References

Álvarez-Errico D, Vento-Tormo R, Sieweke M, Ballestar E. 2014. Epigenetic control of myeloid cell differentiation, identity and function. *Nat Rev Immunol* **15**: 7–17.

Anders S, Huber W. 2010. Differential expression analysis for sequence count data. *Genome Biol* **11**: R106.

Arner E, Daub CO, Vitting-Seerup K, Andersson R, Lilje B, Drabløs F, Lennartsson A, Rönnerblad M, Hrydziuszko O, Vitezic M, et al. 2015. Transcribed enhancers lead waves of coordinated transcription in transitioning mammalian cells. *Science* **347**: 1010–1015.

Austenaa L, Barozzi I, Chronowska A, Termanini A, Ostuni R, Prosperini E, Stewart AF, Testa G, Natoli G. 2012. The Histone Methyltransferase Wbp7 Controls Macrophage Function through GPI Glycolipid Anchor Synthesis. *Immunity* **36**: 572–585.

Barski A, Cuddapah S, Cui K, Roh T-Y, Schones DE, Wang Z, Wei G, Chepelev I, Zhao K. 2007. High-resolution profiling of histone methylations in the human genome. *Cell* **129**: 823–37.

Chen X, Barozzi I, Termanini A, Prosperini E, Recchiuti A, Dalli J, Mietton F, Matteoli G, Hiebert S, Natoli G. 2012. Requirement for the histone deacetylase Hdac3 for the inflammatory gene expression program in macrophages. *Proc Natl Acad Sci U S A* **109**: 2865–2874.

Creyghton MP, Cheng AW, Welstead GG, Kooistra T, Carey BW, Steine EJ, Hanna J, Lodato M a, Frampton GM, Sharp P a, et al. 2010. Histone H3K27ac separates active from poised enhancers and predicts developmental state. *Proc Natl Acad Sci U S A* **107**: 21931–6.

Drouin S, Lame´e L, Jacques P-E´, Forest A, Bergeron M, Robert F. 2010. DSIF and RNA polymerase II CTD phosphorylation coordinate the recruitment of Rpd3S to actively transcribed genes. *PLoS Genet* **6**: 1–12.

Ernst J, Kheradpour P, Mikkelsen TS, Shoresh N, Ward LD, Epstein CB, Zhang X, Wang L, Issner R, Coyne M, et al. 2011. Mapping and analysis of chromatin state dynamics in nine human cell types. *Nature* **473**: 43–9.

Feng J, Liu T, Qin B, Zhang Y, Liu XS. 2012. Identifying ChIP-seq enrichment using MACS. *Nat Protoc* **7**: 1728–40.

Foster SL, Hargreaves DC, Medzhitov R. 2007. Gene-specific control of inflammation by TLR-induced chromatin modifications. *Nature* **447**: 972–8.

Garber M, Yosef N, Goren A, Raychowdhury R, Thielke A, Guttman M, Robinson J, Minie B, Chevrier N, Itzhaki Z, et al. 2012. A High-Throughput Chromatin Immunoprecipitation Approach Reveals Principles of Dynamic Gene Regulation in Mammals. *Mol Cell* **47**: 810–22.

Ghisletti S, Barozzi I, Mietton F, Polletti S, De Santa F, Venturini E, Gregory L, Lonie L, Chew A, Wei C-L, et al. 2010. Identification and characterization of enhancers controlling the inflammatory gene expression program in macrophages. *Immunity* **32**: 317–28.

Greer EL, Shi Y. 2012. Histone methylation: a dynamic mark in health, disease and inheritance. *Nat Rev Genet* **13**: 343–57.

Heinz S, Benner C, Spann N, Bertolino E, Lin YC, Laslo P, Cheng JX, Murre C, Singh H, Glass CK. 2010. Simple combinations of lineage-determining transcription factors prime cis-regulatory elements required for macrophage and B cell identities. *Mol Cell* **38**: 576–89.

Hemmi H, Kaisho T, Takeda K, Akira S. 2003. The Roles of Toll-Like Receptor 9, MyD88, and DNA-Dependent Protein Kinase Catalytic Subunit in the Effects of Two Distinct CpG DNAs on Dendritic Cell Subsets. *J Immunol* **170**: 3059–3064.

Henikoff S. 2008. Nucleosome destabilization in the epigenetic regulation of gene expression. *Nat Rev Genet* **9**: 15–26.

Henikoff S, Shilatifard A. 2011. Histone modification: Cause or cog? *Trends Genet* **27**: 389–396.

Hirotani T, Yamamoto M, Kumagai Y, Uematsu S, Kawase I, Takeuchi O, Akira S. 2005. Regulation of lipopolysaccharide-inducible genes by MyD88 and Toll/IL-1 domain containing adaptor inducing IFN-beta. *Biochem Biophys Res Commun* **328**: 383–392.

Hoshino K, Kaisho T, Iwabe T, Takeuchi O, Akira S. 2002. Differential involvement of IFN- in Toll-like receptor-stimulated dendritic cell activation. *Int Immunol* **14**: 1225–1231.

Illingworth RS, Bird AP. 2009. CpG islands--'a rough guide'. *FEBS Lett* **583**: 1713–20.

Ivashkiv LB, Park SHO. 2016. Epigenetic Regulation of Myeloid Cells. *Microbiol Spectr* **4**.

Kaikkonen MU, Spann NJ, Heinz S, Romanoski CE, Allison K a, Stender JD, Chun HB, Tough DF, Prinjha RK, Benner C, et al. 2013. Remodeling of the enhancer landscape during macrophage activation is coupled to enhancer transcription. *Mol Cell* **51**: 310–25.

Kawai T, Akira S. 2010. The role of pattern-recognition receptors in innate immunity: update on Toll-like receptors. *Nat Immunol* **11**: 373–84.

Kayama H, Ramirez-Carrozzi VR, Yamamoto M, Mizutani T, Kuwata H, Iba H, Matsumoto M, Honda K,

Smale ST, Takeda K. 2008. Class-specific regulation of pro-inflammatory genes by MyD88 pathways and IκBζ. *J Biol Chem* **283**: 12468–12477.

Kim D, Pertea G, Trapnell C, Pimentel H, Kelley R, Salzberg SL. 2013. TopHat2: accurate alignment of transcriptomes in the presence of insertions, deletions and gene fusions. *Genome Biol* **14**: R36.

Kumagai Y, Vandenbon A, Teraguchi S, Akira S, Suzuki Y. Genome-wide map of RNA degradation kinetics patterns in dendritic cells after LPS stimulation facilitates identification of primary sequence and secondary structure motifs in mRNAs. *BMC Genomics* in press.

Langmead B, Salzberg SL. 2012. Fast gapped-read alignment with Bowtie 2. *Nat Methods* **9**: 357–9.

Law CW, Chen Y, Shi W, Smyth GK. 2014. voom : precision weights unlock linear model analysis tools for RNA-seq read counts. 1–17.

Lee B, Bhinge AA, Battenhouse A, Song L, Zhang Z, Grasfeder LL, Mcdaniell RM, Liu Z, Ni Y, Birney E, et al. 2012. Cell-type specific and combinatorial usage of diverse transcription factors revealed by genome-wide binding studies in multiple human cells. *Genome Res* **22**: 9–24.

Lenhard B, Sandelin A, Carninci P. 2012. Metazoan promoters: emerging characteristics and insights into transcriptional regulation. *Nat Rev Genet* **13**: 233–45.

Li H, Handsaker B, Wysoker A, Fennell T, Ruan J, Homer N, Marth G, Abecasis G, Durbin R. 2009. The Sequence Alignment/Map format and SAMtools. *Bioinformatics* **25**: 2078–9.

Liang K, Suzuki Y, Kumagai Y, Nakai K. 2014. Analysis of changes in transcription start site distribution by a classification approach. *Gene* **537**: 29–40.

Lim CA, Yao F, Wong JJY, George J, Xu H, Chiu KP, Sung WK, Lipovich L, Vega VB, Chen J, et al. 2007. Genome-wide Mapping of RELA(p65) Binding Identifies E2F1 as a Transcriptional Activator Recruited by NF-κB upon TLR4 Activation. *Mol Cell* **27**: 622–635.

MacQuarrie KL, Fong AP, Morse RH, Tapscott SJ. 2011. Genome-wide transcription factor binding: beyond direct target regulation. *Trends Genet* **27**: 141–148.

Mercer EM, Lin YC, Benner C, Jhunjhunwala S, Dutkowski J, Flores M, Sigvardsson M, Ideker T, Glass CK, Murre C. 2011. Multilineage priming of enhancer repertoires precedes commitment to the B and myeloid cell lineages in hematopoietic progenitors. *Immunity* **35**: 413–25.

Meyer LR, Zweig AS, Hinrichs AS, Karolchik D, Kuhn RM, Wong M, Sloan C a, Rosenbloom KR, Roe G, Rhead B, et al. 2013. The UCSC Genome Browser database: extensions and updates 2013. *Nucleic Acids Res* **41**: D64–9.

Miller T, Krogan NJ, Dover J, Tempst P, Johnston M, Greenblatt JF, Sherman DR, Voskuil M, Schnappinger D, Harrell MI, et al. 2001. COMPASS: A complex of proteins associated with a trithorax-related SET domain protein. *Proc Natl Acad Sci U S A* **98**: 12902–12907.

Mortazavi A, Williams B a, McCue K, Schaeffer L, Wold B. 2008. Mapping and quantifying mammalian transcriptomes by RNA-Seq. *Nat Methods* **5**: 621–8.

Natoli G. 2009. Control of NF- k B-dependent Transcriptional Responses by Chromatin Organization. *Cold Spring Harb Perspect Biol* **1**: 1–11.

Ostuni R, Piccolo V, Barozzi I, Polletti S, Termanini A, Bonifacio S, Curina A, Prosperini E, Ghisletti S, Natoli G. 2013. Latent enhancers activated by stimulation in differentiated cells. *Cell* **152**: 157–71.

Patil A, Kumagai Y, Liang K-C, Suzuki Y, Nakai K. 2013. Linking transcriptional changes over time in stimulated dendritic cells to identify gene networks activated during the innate immune response. *PLoS Comput Biol* **9**: e1003323.

Pavri R, Zhu B, Li G, Trojer P, Mandal S, Shilatifard A, Reinberg D. 2006. Histone H2B Monoubiquitination Functions Cooperatively with FACT to Regulate Elongation by RNA Polymerase II. *Cell* **125**: 703–717.

Qiao Y, Giannopoulou EG, Chan CH, Park S-H, Gong S, Chen J, Hu X, Elemento O, Ivashkiv LB. 2013. Synergistic activation of inflammatory cytokine genes by interferon-γ-induced chromatin

remodeling and toll-like receptor signaling. *Immunity* **39**: 454–69.

Rabani M, Raychowdhury R, Jovanovic M, Rooney M, Stumpo DJ, Pauli A. 2014. Resource High-Resolution Sequencing and Modeling Identifies Distinct Dynamic RNA Regulatory Strategies. *Cell* **159**: 1698–1710.

Ramana C V, Chatterjee-Kishore M, Nguyen H, Stark GR. 2000. Complex roles of Stat1 in regulating gene expression. *Oncogene* **19**: 2619–2627.

Saitoh T, Satoh T, Yamamoto N, Uematsu S, Takeuchi O, Kawai T, Akira S. 2011. Antiviral protein viperin promotes toll-like receptor 7- and toll-like receptor 9-mediated type i interferon production in plasmacytoid dendritic cells. *Immunity* **34**: 352–363.

Schübeler D, MacAlpine DM, Scalzo D, Wirbelauer C, Kooperberg C, Van Leeuwen F, Gottschling DE, O'Neill LP, Turner BM, Delrow J, et al. 2004. The histone modification pattern of active genes revealed through genome-wide chromatin analysis of a higher eukaryote. *Genes Dev* **18**: 1263–1271.

Smale ST, Tarakhovsky A, Natoli G. 2014. Chromatin contributions to the regulation of innate immunity. *Annu Rev Immunol* **32**: 489–511.

Stasevich TJ, Hayashi-Takanaka Y, Sato Y, Maehara K, Ohkawa Y, Sakata-Sogawa K, Tokunaga M, Nagase T, Nozaki N, McNally JG, et al. 2014. Regulation of RNA polymerase II activation by histone acetylation in single living cells. *Nature* **516**: 272–5.

Tartey S, Matsushita K, Vandenbon A, Ori D, Imamura T, Mino T, Standley DM, Hoffmann JA, Reichhart J, Akira S. 2014. Akirin 2 is critical for inducing inflammatory genes by bridging IκB-ζ and the SWI / SNF complex. *EMBO J* **33**: 2332–2348.

Toshchakov V, Jones BW, Perera P-Y, Thomas K, Cody MJ, Zhang S, Williams BRG, Major J, Hamilton T a, Fenton MJ, et al. 2002. TLR4, but not TLR2, mediates IFN-beta-induced STAT1alpha/beta-dependent gene expression in macrophages. *Nat Immunol* **3**: 392–8.

Tsuchihara K, Suzuki Y, Wakaguri H, Irie T, Tanimoto K, Hashimoto S, Matsushima K, Mizushima-Sugano J, Yamashita R, Nakai K, et al. 2009. Massive transcriptional start site analysis of human genes in hypoxia cells. *Nucleic Acids Res* **37**: 2249–63.

Vahedi G, Takahashi H, Nakayamada S, Sun H, Sartorelli V, Kanno Y, O'Shea JJ. 2012. STATs Shape the Active Enhancer Landscape of T Cell Populations. *Cell* **151**: 981–993.

Voss TC, Hager GL. 2014. Dynamic regulation of transcriptional states by chromatin and transcription factors. *Nat Rev Genet* **15**: 69–81.

Weiner A, Hsieh T-HS, Appleboim A, Chen H V, Rahat A, Amit I, Rando OJ, Friedman N. 2015. High-Resolution Chromatin Dynamics during a Yeast Stress Response. *Mol Cell* **58**: 371–386.

Weintraub H, Groudine M. 1976. Chromosomal Subunits in Active Genes Have an Altered Conformation. *Science* **193**: 848–856.

Winter DR, Amit I. 2014. The role of chromatin dynamics in immune cell development. *Immunol Rev* **261**: 9–22.

Yamamoto M, Sato S, Hemmi H. 2003. Role of Adaptor TRIF in the MyD88-Independent Toll-Like Receptor Signaling Pathway. *Science* **301**: 640–643.

Zhu Y, van Essen D, Saccani S. 2012. Cell-Type-Specific Control of Enhancer Activity by H3K9 Trimethylation. *Mol Cell* **46**: 408–423.